

SYNTHESIS AND SPECTROSCOPIC STUDY OF Si, Ti, Mg, AND Zn OXIDES MODIFIED BY L-PROLINE

O. V. Koryakova,^a M. S. Valova,^{a,*} Yu. A. Titova,^a
A. N. Murashkevich,^b and O. V. Fedorova^a

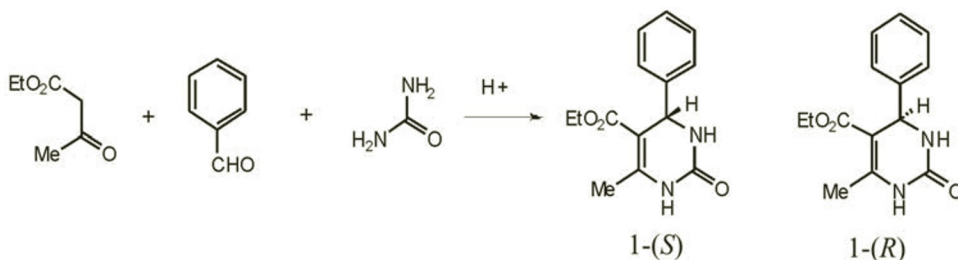
UDC 544.723.5+542.8

*Individual and mixed oxides of Zn, Mg, Si, and Ti modified with L-proline during their sol-gel synthesis have been obtained. The IR spectra of these oxides studied in detail show changes in the vibrational band parameters of the siliconoxygen and metal–oxygen bonds. Enhancement of the amount of basic sites on the SiO₂–TiO₂ mixed oxide was found after removal of L-proline from the surface. The use of SiO₂–Mg(OH)₂*L-proline composite as a catalyst leads to an enhanced enantiomeric excess of some asymmetric Biginelli reaction products up to 18%.*

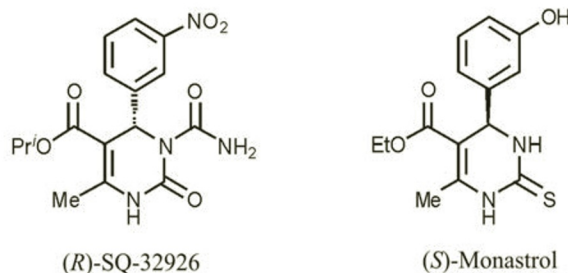
Keywords: sol-gel synthesis, IR spectroscopy, oxides of silicon, zinc, magnesium, and titanium, composites with L-proline, adsorption, catalysts, Biginelli reaction, active centers.

Introduction: Metal oxides are commonly used as catalysts in organic synthesis both in industry and laboratory practice [1]. The nature of the catalytically active sites of the surface of oxide catalysts has been studied in detail [2–6]. The catalytic activity of a heterogeneous catalyst entailing increased reaction rate, selectivity, and yield of the desired product depends on the amount and nature of the active sites participating in the catalytic reaction [4]. The use of IR spectroscopy in the study of heterogeneous catalysts provides information on the presence and nature of the active sites on the inorganic oxide surface and on the intermolecular and chemical reactions of organic molecules with the catalyst as well as pointing to a mechanism of their catalytic action [7, 8]:

In the present work, we studied metal oxides and silicon oxide as catalysts of the Biginelli reaction [7, 9]:



leading to the formation of 1,4-dihydropyrimidines (DHPM) possessing cardiotropic, hypotensive, and antitumor, and antiviral activity [10]:



*To whom correspondence should be addressed.

^aPostovsky Institute of Organic Synthesis, Ural Branch of the Russian Academy of Sciences, 620990, Yekaterinburg, Russia; email: vms@ios.uran.ru; ^bBelarusian State Technological University, Minsk, Belarus. Translated from Zhurnal Prikladnoi Spektroskopii, Vol. 88, No. 3, pp. 398–407, May–June, 2021. Original article submitted March 3, 2020.

DHPM have traditionally been obtained as a mixture of (*S*)- and (*R*)-enantiomers in 1:1 ratio (nonsymmetric Biginelli reaction); these two enantiomers can differ significantly in their pharmacological activity. For example, the (*R*)-enantiomer of SQ 32926 displays 400 times greater hypotensive activity than the (*S*)-enantiomer [11]. Similarly, the inhibitory activity of (*S*)-monastrol toward mitotic kinesin Eg5 is 15 times greater than the corresponding activity of (*R*)-monastrol [12].

Various classes of chiral inducers are being studied in the search for new approaches to the synthesis of enantiomerically pure DHPM or samples at least enriched in one of the enantiomers (asymmetric Biginelli reaction) [13].

L-Proline is an important amino acid commonly used to increase the stereoselectivity in organic synthesis such as the asymmetric Biginelli reaction [14–16]. In the previous work [7], we showed that individual Zn, Mg, and Ti oxides enhance the stereocatalytic activity of *L*-proline in the asymmetric Biginelli reaction. *L*-Proline [17, 18], zinc *L*-prolinate [19] as well as *L*-proline sulfate adsorbed on the silica gel surface [20] were found to enhance the chemoselectivity of the Biginelli reaction when used to catalyze the nonsymmetric reaction.

The immobilization of *L*-proline on inorganic supports including mesoporous materials has been studied by Bae et al. [21, 22]. The adsorption of *L*-proline on anionic clays yields an efficient heterogeneous catalyst for the asymmetric aldol condensation [23]. There have been no reports of the use of *L*-proline adsorbed on synthetic inorganic oxides in asymmetric reactions. Composites derived from *L*-proline and inorganic oxides obtained by solgel synthesis have not been described in the literature. On the other hand, greater amounts of active acidic and basic sites on oxide catalysts have been found after increasing the surface area of these oxides or by modification of their surface. For example, Tanabe [6] has described a change in the acidity of the surface of oxides upon adsorption of fluoride or sulfate. The effect of amino acids supported on the surface of oxides on the amount and nature of the active sites has not been studied.

In the present work, we prepared individual and mixed Zn, Mg, Si, and Ti oxides modified by *L*-proline during solgel synthesis, carried out a detailed IR spectroscopic study of these oxides, in particular, discovered changes in the spectral characteristics of bonds linking the oxides and *L*-proline, investigated the effect of *L*-proline on the amount of basic active sites, and also studied these composites as catalysts for the asymmetric Biginelli reaction.

Experimental. *Synthesis of ZnO (sample 1).* The numbering and characteristics of this sample are given in Table 1. A 0.45 M solution of zinc nitrate (132 mL) was added dropwise to 560 mL 0.43 M aqueous sodium hydroxide. The sodium hydroxide solution was taken in two-fold molar excess. The suspension was stirred and the resultant zinc hydroxide precipitate was maintained in the mother liquor for 24 h followed by filtration and then washing with 0.7 L distilled water. The precipitate obtained was heated to 120°C in an autoclave at a rate of 0.5°C/min, maintained at this temperature for 1 h, and rapidly cooled to room temperature to give a powder of crystalline zinc oxide (sample 1) with zincite structure and crystallite diameter 20–40 nm, which is in good accord with the estimation of particle size by calculation using the specific surface [24].

Synthesis of MgO and SiO₂-MgO (samples 4 and 5). A sample of magnesium sample was precipitated from a solution of magnesium sulfate by adding 24% ammonium hydroxide and then maintained at room temperature. The product was filtered and washed to remove sulfate ions followed by heat treatment at 400°C for 1 h to give crystalline magnesium oxide powder with platelet particles (sample 4) [25]. In order to obtain SiO₂-MgO (sample 5), a sol of silicon dioxide was first obtained. Calcium carbonate was added to a beaker and water was added. The mixture was stirred for 10 min and H₂SiF₆ at pH 5.1–5.3 was added dropwise using a separatory funnel. The solid CaF₂ phase was separated from the liquid SiO₂ sol phase by centrifugation. A sample of magnesium oxide was precipitated separately from a solution of magnesium sulfate by adding 24% ammonium hydroxide, maintained at room temperature, filtered, and washed to remove sulfate ions. The SiO₂ sol and magnesium hydroxide were mixed and heated at 400°C for 1 h (sample 5). Both magnesium hydroxide with brushite structure and nanocrystalline magnesium oxide were found in the SiO₂-MgO product.

The synthesis of SiO₂-TiO₂ (sample 8) was carried out according to reported procedures [26, 27].

*Synthesis of inorganic oxide*L-proline composites (samples 2, 6, 9) and composites with the L-proline footprint (samples 3, 7, 10).* Composites with *L*-proline were synthesized by adding this compound during the solgel synthesis of oxides with 1:1 mass ratio of the individual or mixed oxide and *L*-proline according to our previous work [24]. Each sample was divided into two parts. One part of the product was dried at 110°C for 2 h to give composites 2, 6, and 9 (inorganic oxide*L-proline, unwashed). The second half was thoroughly washed with water and dried at 110°C to constant mass to give composites of the inorganic oxide with an *L*-proline footprint (inorganic oxide*L-proline, washed, samples 3, 7, and 10). A solution of the modifier was introduced in the initial stage of the synthesis. Then, the resultant double oxide was filtered such that a part of the organic modifier was removed with the filtrate. In contrast to the starting oxides (samples 1, 4, 5, and 8), these composite powders of inorganic oxide*L-proline (samples 2, 3, 6, 7, 9, and 10) are amorphous since they were not calcined.

TABLE 1. Composition of the Composites, Their Specific Surface, and Amount of Basic Active Sites (n_c)

Sample	Composition	S_{sp} , m ² /g	n_c , mmole-eq/g	<i>L</i> -proline content, %	Elemental analysis data (CHN), %			
					C	H	N	MeO _x
1	ZnO	46	0.269	0.0	0.44	0.42	none	96.93
2	ZnO* <i>L</i> -proline, unwashed	–	0.252	51.4	30.95	4.02	7.16	42.87
3	ZnO* <i>L</i> -proline, washed	40	0.152	0.0	0.53	none	none	98.34
4	MgO	394	–	0.0	4.12	2.77	none	64.57
5	SiO ₂ –MgO (50:50)	367	0.218	0.0	1.36	2.45	none	77.51
6	SiO ₂ –Mg(OH) ₂ (50:50)* <i>L</i> -proline, unwashed	–	0.363	46.2	24.09	5.25	5.65	44.07
7	SiO ₂ –Mg(OH) ₂ (50:50)* <i>L</i> -proline, washed	261	0.734	0.0	0.63	2.33	none	80.14
8	SiO ₂ –TiO ₂ (82:18)	271	0.072	0.0	0.61	1.30	none	82.85
9	SiO ₂ –TiO ₂ (82:18)* <i>L</i> -proline, unwashed	–	0.297	36.6	19.12	3.64	4.76	58.06
10	SiO ₂ –TiO ₂ (82:18)* <i>L</i> -proline, washed	282	0.565	1.4	0.71	1.75	1.05	84.09

Adsorption of L-proline on MgO and on SiO₂–MgO (samples 4a and 5a). Samples 4a and 5a were obtained by the adsorption of *L*-proline from ethanolic solution with 1:3 adsorbate:adsorbent molar ratio followed by removal of the solvent at 60–70°C.

Research methods. The specific surface was measured by the adsorption method from a solution in heptane using phenol as the adsorbate [28]. The amount of active sites (n_c) was determined by titration of residual benzoic acid (from a 0.01 N solution in cyclohexane) after adsorption of this acid on the sample surface using a solution of potassium hydroxide [29]. The composites were studied by diffuse reflection IR spectroscopy since this method yields the most precise data on the vibrations of surface-adsorbed compounds. The spectra were taken on a Perkin Elmer Spectrum One spectrometer at 4000–370 cm⁻¹ using an automatic console. The C, H, N mass fractions (%) were determined using an automatic Perkin Elmer PE-2400, series II CHN analyzer. The dynamic radius and size distribution of the composite particles in aqueous solution were found by dynamic light scattering using a Brookhaven Instruments Zeta Plus universal analyzer. The mass fractions of silicon and titanium were determined by atomic emission spectroscopy (AES) on a Thermo Scientific iCAP6300 Duo inductively-coupled plasma-optical emission spectrometer (manufactured in the USA). The morphology of the samples was analyzed by scanning electron microscopy (SEM) using a Carl Zeiss Merlin electron microscope (manufactured in Germany).

The asymmetric Biginelli reaction was carried out in the presence of 10 mole % chiral inducer and/or 10 mole % oxide catalyst. The enantiomeric excesses (*ee*) were determined by high-efficiency liquid chromatography using YMC-Pack and Chiral-NEA-R; the elution was carried out with 35:65 CH₃CN–H₂O.

Results and Discussion. The elemental AES analysis showed that the actual SiO₂:TiO₂ ratio was similar to the calculated value. Washing the composite to remove the *L*-proline organic phase did not lead to removal of the inorganic components. Thus, for sample 9, [SiO₂] = 41.2% and [TiO₂] = 9.82%, while for sample 10, [SiO₂] = 63.6% and [TiO₂] = 16.5%

According to the SEM data, the SiO₂–TiO₂**L*-proline composites (samples 9 and 10) are amorphous powders consisting of irregularly-shaped aggregates with mean diameter 500–600 nm (sample 9) and 250–350 nm (sample 10). The aggregates consist of small flakes with diameter ~15–40 nm (Fig. 1).

Dynamic light scattering was used to determine the dynamic radii and size distribution of the component particles in aqueous solution. The particles in all the samples were found to be aggregates with diameters 2558 ± 276 nm for unwashed ZnO**L*-proline (sample 2), 2240 ± 238 nm after washing (sample 3), 3176 ± 238 nm for unwashed SiO₂–Mg(OH)₂**L*-pro-

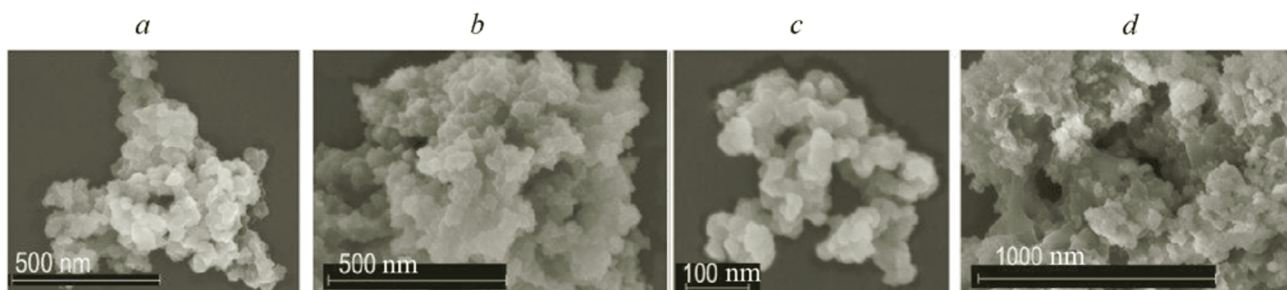


Fig. 1. SEM images of particles of composites 9 (a, b) and 10 (c, d).

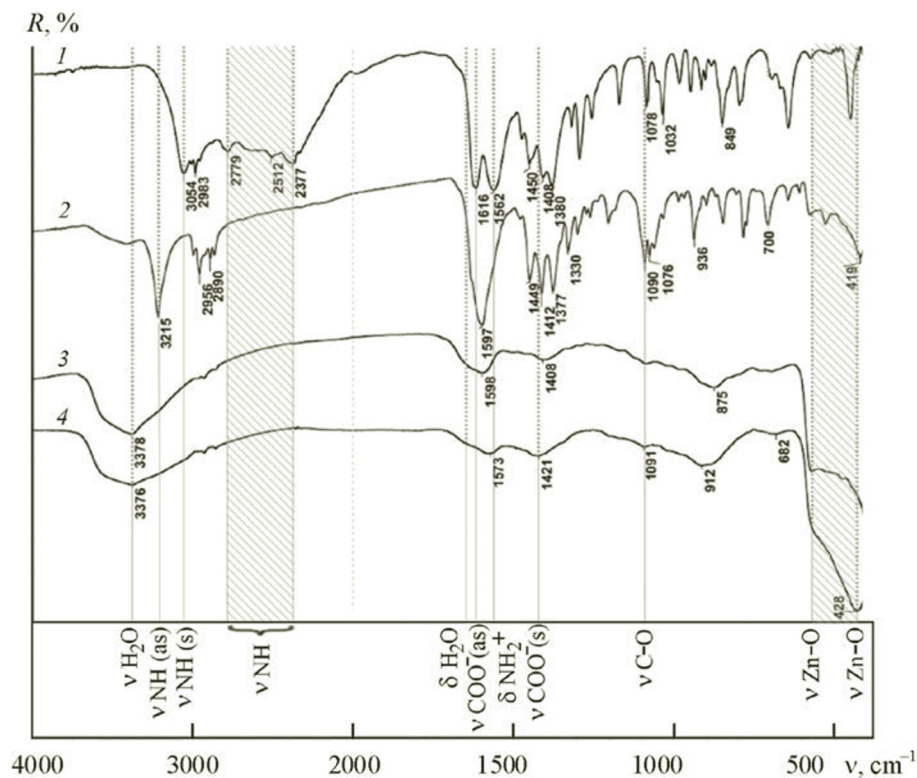


Fig. 2. IR spectra of *L*-proline (1) and samples 2 (2), 3 (3), and 4 (4).

line (sample 6), 1443 ± 46 nm after washing (sample 7), 339 ± 8 nm for $\text{SiO}_2\text{-TiO}_2^*L\text{-proline}$ (sample 9), 557 ± 36 nm after washing (sample 10). These values are in accord with the SEM data (Fig. 1).

The CHN elemental analysis data were used to calculate the amount of *L*-proline in these samples (Table 1). The amount of *L*-proline in the composites obtained by sol-gel synthesis decreases in the series $\text{ZnO} \gg \text{SiO}_2\text{-Mg(OH)}_2 > \text{SiO}_2\text{-TiO}_2$. The amount of *L*-proline adsorbed on $\text{SiO}_2\text{-MgO}$ (sample 5a) is less than 9%, which is five times less than for composite 6.

After washing the composites with water, *L*-proline was almost entirely removed from the oxides with the exception of $\text{SiO}_2\text{-TiO}_2$, on which 1.4% *L*-proline remains. This finding can be attributed to the circumstance that titanium oxide and silicon oxide have the strongest bonding to *L*-proline (samples 3, 7, and 10).

In previous work [7, 9], we used IR spectroscopy to show that the catalysis of the

Biginelli reaction by metal oxides or silicon oxide is due to activation of the organic compounds after their adsorption on the catalyst surface. An important role was found for activated molecules of water and carbon dioxide on the oxide surface. In the present work, we studied the IR spectra of some inorganic oxide**L*-proline composites.

The diffuse reflection IR spectrum of the sample used of *L*-proline at $400\text{-}2000$ cm^{-1} hardly differs from the corresponding spectrum of the solid sample [30] prepared by pressing with potassium bromide. The band at 3050 cm^{-1} and the

broad absorption with maxima at 2779, 2512, and 2396 cm^{-1} , indicating strong hydrogen bonding, should be ascribed to N–H bond stretching vibrations. The absorption bands at 1616 and 1408 cm^{-1} as well as at 1562 and 1380 cm^{-1} characterize vibrations of the COO^- and NH_2^+ groups, respectively, and indicate that this molecule is present as a zwitterion (Fig. 2, curve 1) [30, 31].

The vibrations of the Zn–O bonds in zinc oxide (sample 1) are seen as a broad band with a maximum near 430 cm^{-1} and a shoulder at 550 cm^{-1} (Fig. 2, curve 4) [32, 33]. Furthermore, a series of weak washedout bands is seen at 700–1200 cm^{-1} , which can be assigned to ZnO bond vibrations on the surface, where the Zn^{2+} cation is incompletely coordinated (800–1200 cm^{-1}) [4], multiphonic vibrations of the Zn–O lattice (700–1100 cm^{-1}) [34], and deformation vibrations of the surface Zn–O–H bonds (833–850 cm^{-1}) [33]. The bands at 3376 and 1630 cm^{-1} indicate the presence of water. The spectrum also shows a weak absorption with a maximum at 1421 cm^{-1} , corresponding to carbonate ions related to carbon dioxide on the oxide surface [3].

The maximum of the band for the vibrations of the Zn–O bonds in the spectrum of sample is 9 cm^{-1} less than for pure ZnO. Changes in the *L*-proline bands (Fig. 2, curves 1 and 2) also indicate a weak interaction of the components. Firstly, the absorption of the zwitterion NH_2^+ group at 3050 and 2300–2600 cm^{-1} is absent in the spectrum of composite 2 and a band for the stretching vibrations of the secondary N–H bond appears at 3215 cm^{-1} [31]. Secondly, there are no NH_2^+ group deformation bands (1562 cm^{-1}). The deformation vibrational band for the secondary amino group formed upon decomposition of the zwitterion has low intensity [35] and overlaps the band for the ionized carboxyl group at 1597 cm^{-1} [36]. These findings confirm the decomposition of the zwitter-ion NH_2^+ group and formation of a complex of the amino acid with the metal. Hence, we can presume that the coordination of *L*-proline in the unwashed metal-O**L*-proline composites is a chelate-like structure analogous to that described for copper proline, $\text{Cu}(\text{L-proline})_2$ [30] and zinc proline, $\text{Zn}(\text{L-proline})_2$ [37]. Washing leads to the disappearance of the *L*-proline bands in the spectrum of the ZnO**L*-proline composite (sample 3) (curve 3), which indicates the decomposition of the complex and washingout of *L*-proline. The frequency of the vibrations of the Zn–O bonds is shifted below 400 cm^{-1} and a maximum appears at 550 cm^{-1} instead of a shoulder. The displacement in the region of the vibrations of the surface Zn–O bonds toward lower frequencies (from 912 to 875 cm^{-1}) indicates a change in the parameters of the Zn–O bond after the removal of *L*-proline and may be a consequence of formation of a footprint of the *L*-proline molecule (sample 1).

The IR spectrum of magnesium oxide (Fig. 3, curve 3) shows a broad absorption corresponding to Mg–O bond vibrations at 500–680 cm^{-1} , water absorption bands (ν -3392 cm^{-1} and δ -1642 cm^{-1}), and broad bands with maxima at 1418 and 1091 cm^{-1} , indicating the formation of monodentate carbonate complexes on the surface [36] due to the adsorption of carbon dioxide. The adsorption of *L*-proline on magnesium oxide (sample 4a) leads to disappearance of the zwitterion absorption bands and the appearance of amino group bands at 3223 and 1596 cm^{-1} (curve 4) on the background of carbonate ion and water bands. The latter coalesces with the band of the ionized carboxyl group, whose frequency is reduced probably due to interaction with the metal. At the same time, the maximum of the second band of this group at 1380 cm^{-1} is shifted toward higher frequencies. Thus, the IR spectrum of the product of the adsorption of *L*-proline on MgO indicates that even under mild conditions, the components interact to form magnesium *L*-proline by analogy to composite 2.

The vibrations of the Si–O bonds in the spectrum of sample 5 (Fig. 3, curve 2) appear at 64 cm^{-1} lower (1015 cm^{-1}) than in the spectrum of silicon nanooxide (curve 1) described in our previous work [26]. This finding as well as the lack of strong absorption at 500–680 cm^{-1} of the Mg–O–Mg bonds in magnesium oxide may be considered as additional evidence for the formation of Si–O–Mg bonds formed upon heat treatment at 400°C. The spectrum has water absorption bands (ν -3390 cm^{-1} and δ -1633 cm^{-1}), whose intensity is much less than for the element–oxygen bond vibrational bands in the spectrum of MgO. The weak absorption with maximum at 1423 cm^{-1} indicates the presence of trace amounts of carbonate groups [27] (curve 2).

L-Proline adsorbed on the SiO_2 –MgO composite prepared at 400°C gives rise to weak bands in the IR spectrum of sample 5a, which indicates a much smaller amount of this compound than in the case of MgO. The *L*-proline absorption bands at 1616 and 1562 cm^{-1} (Fig. 3, curve 2) are different in frequency and shape and overlap the water deformation vibration band (curves 5 and 7). The superposition of these bands is seen near 1625 cm^{-1} . The maxima of the complex band at 1300–1410 cm^{-1} are shifted toward higher frequencies to 1387 and 1421 cm^{-1} . The zwitter-ion bands at 2300–2700 and 3050 cm^{-1} are not found in the spectrum of this sample while the band for the N–H bonds is not seen on the background of the strong band for O–H bond stretching vibrations, whose maximum is shifted somewhat toward lower frequencies (3378 cm^{-1}) relative to sample 5 (curve 2). The adsorption of *L*-proline presumably takes place predominantly on the magnesium cation.

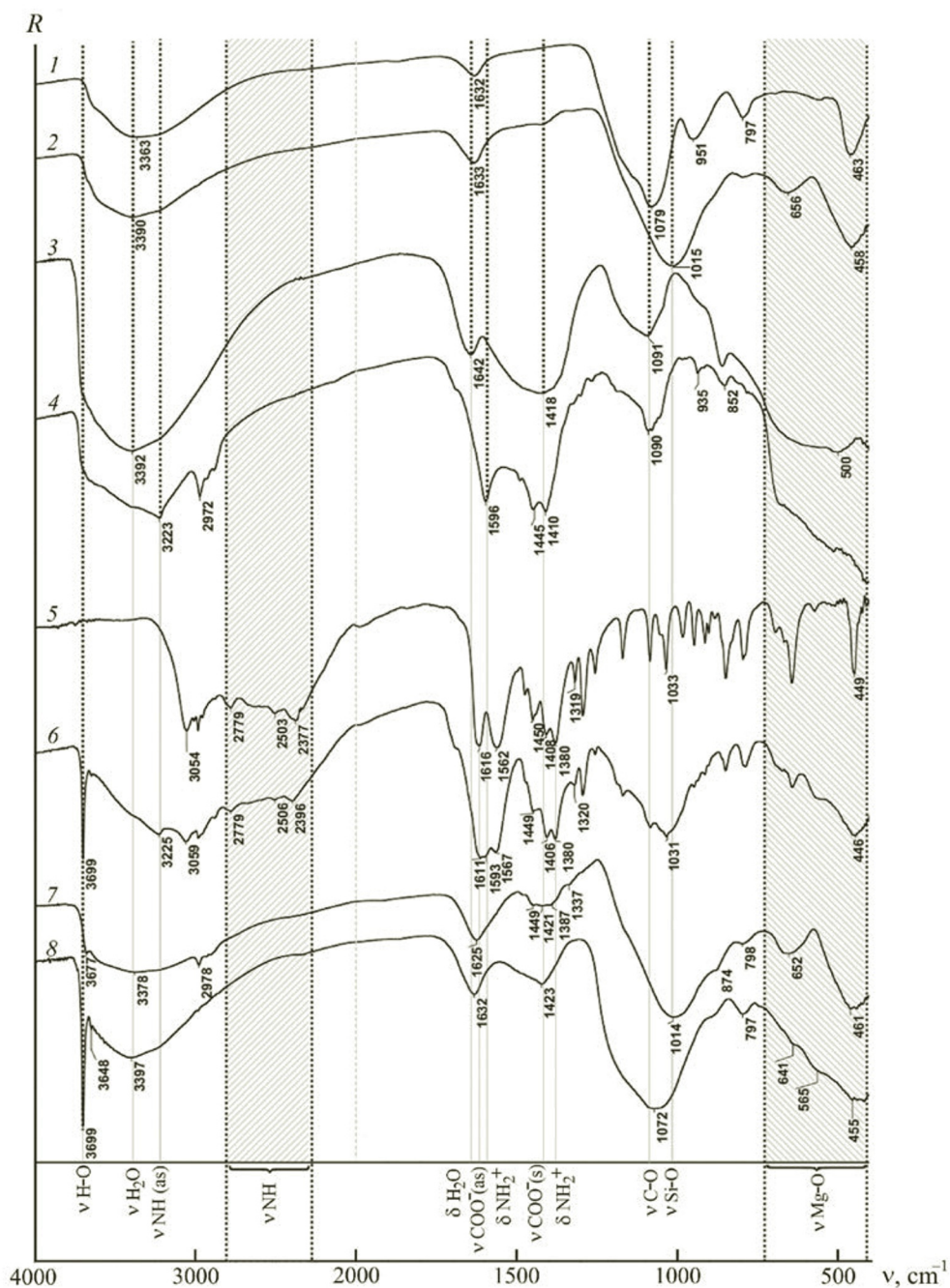


Fig. 3. IR spectra of SiO_2 (1), samples 5 (2), 4 (3), 6 (6), 7 (8), L -proline (5); adsorption of L -proline on MgO (sample 4a) (4) and on $\text{SiO}_2\text{-Mg-O}$ (sample 5a) (7).

The IR spectrum of composite 6 has bands for the stretching vibrations of the N-H bonds of the hydrogenbonded primary amino groups (3225 cm^{-1}). The νNH_2^+ bands are shifted and have lower intensity in comparison with pure L -proline (3059 , 2779 , and 2396 cm^{-1}). The bands for the ionized carboxyl group and NH_2^+ deformation vibrations are slightly broader with a shift to 1611 and 1567 cm^{-1} . Along with the band for the Mg-O-Si bond shifted by $\sim 20 \text{ cm}^{-1}$ (1031 cm^{-1}) toward higher frequencies (Fig. 3, curves 2 and 6), there is also a broad band at $\sim 450 \text{ cm}^{-1}$ with a shoulder at 570 cm^{-1} corresponding to MgO vibrations in $\text{Mg}(\text{OH})_2$ [38] as well as a narrow band at 3699 cm^{-1} for the free hydroxyl groups of $\text{Mg}(\text{OH})_2$. The presence of $\text{Mg}(\text{OH})_2$ in sample 6 is probably due to lack of sufficient heat treatment (400°C) in comparison with the heat treatment carried out in the preparation of composite 5 ($\text{SiO}_2\text{-Mg}$). The $\text{SiO}_2\text{-Mg}(\text{OH})_2^*L$ -proline composite

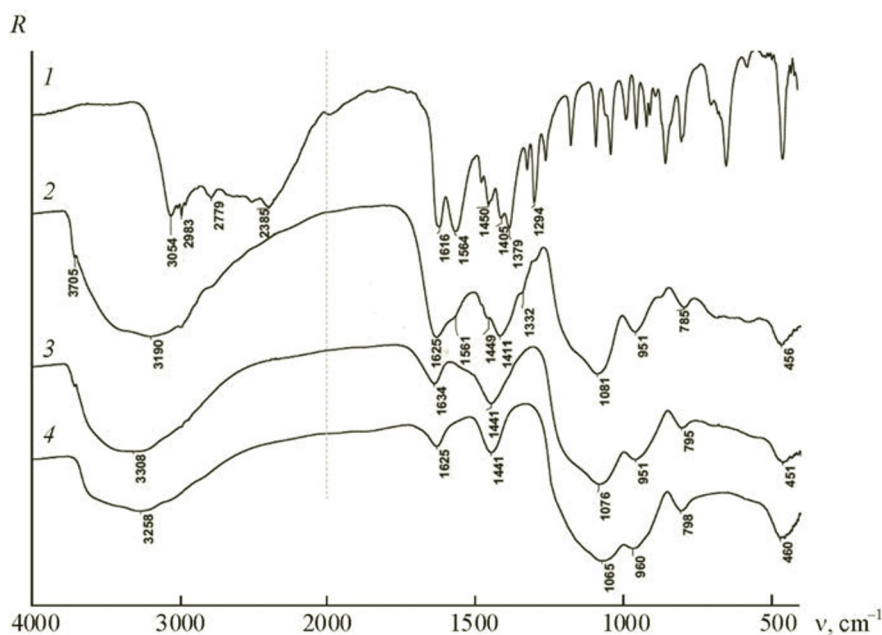


Fig. 4. IR spectra of *L*-proline (1) and samples 9 (2), 10 (3), and 8 (4).

is partially formed upon drying of a mixture of $\text{Mg}(\text{OH})_2$, SiO_2 , and *L*-proline at 110°C . A significant part of the *L*-proline is present in the mixed oxide phase and has distorted structure, as indicated by some change in its spectral characteristics.

The maximum of the absorption band for the Si–O bonds at 1072 cm^{-1} in the IR spectrum of sample 7 corresponds to the maximum of this band in pure silicon oxide [27] (Fig. 4, curve 8). An absorption band for the stretching vibrations of the hydroxyl groups in $\text{Mg}(\text{OH})_2$ is clearly seen at 3699 cm^{-1} [34, 35]. Spectral evidence for the Mg–O–Si bond was not found.

Thus, washing the mixture of SiO_2 , $\text{Mg}(\text{OH})_2$, and *L*-proline (sample 7) without the corresponding heat treatment (110°C) is not accompanied by formation of the $\text{SiO}_2\text{--Mg--O}^*\text{L}$ -proline composite. The $\text{SiO}_2\text{--Mg}(\text{OH})_2^*\text{L}$ -proline composite is obtained only upon drying of a mixture of $\text{Mg}(\text{OH})_2$, SiO_2 , and *L*-proline. The Mg–O bond participates in the coordination of the carboxyl and NH groups of *L*-proline and a structure analogous to that for the ZnO^*L -proline composite is formed. For the mixed oxide $\text{SiO}_2\text{--Ti--O}_2$ (sample 8), the positions of the maxima of the absorption bands of the Si–O–Si and Si–O–Ti bonds in the IR spectrum and specific surface are almost identical to the values given in our previous work [27].

The elemental analysis indicated that sample 9 contains 36.6% *L*-proline (Table 1). The shape and frequency of the *L*-proline bands are significantly altered (Fig. 4, curve 2). The bands of the ionized carboxyl group at 1616 cm^{-1} and the zwitter-ion at 1564 cm^{-1} overlap the water band and are seen as a broad complex band with maximum at 1625 cm^{-1} . The changes at $1300\text{--}1450\text{ cm}^{-1}$ are especially striking: the frequencies of the complex band are shifted and a band appears at 1411 cm^{-1} . The area under the curve and the maximum of the band for vibrations of the O–H bonds (3190 cm^{-1}) also changes and a weak band for the free Si–O–H groups appears at 3705 cm^{-1} . The band for the vibrations of the Si–O–Ti bonds at 960 cm^{-1} is shifted toward lower frequencies to 951 cm^{-1} along with the band for the Si–O–Si bond vibrations, which is shifted toward higher frequency from 1065 to 1081 cm^{-1} . These findings suggest decomposition of the zwitter-ion and formation of a coordination bond of *L*-proline predominantly with the titanium atoms in the composite.

The complex is partially retained in sample 10 after washing as indicated by the shape and stronger intensity of the band at 1441 cm^{-1} relative to the bands for water and the Si–O bonds (Fig. 4, curves 3 and 4). The presence of residual *L*-proline in sample 10 is supported by the elemental analysis data (Table 1).

Thus, the modification of the oxides by *L*-proline molecules during the sol-gel synthesis is accompanied by marked changes in the spectral characteristics of the oxygen–metal bonds, which are retained after the removal of *L*-proline from the surface. This finding may be related to the formation of the *L*-proline molecule footprint.

The amount of active sites in the oxide**L*-proline composites and their specific surface are given in Table 1. The modification of all these oxides by *L*-proline molecules has virtually no effect on the specific surface of the composite but leads to an increased amount of active basic sites in the composites with the exception of ZnO. More than tripling of the

TABLE 2. Stereoselectivity of the Biginelli Reaction

Experiment No.	Oxide or composite	Catalyst	ee, %
1	–	<i>L</i> -proline	11 (<i>S</i>)
2	ZnO (1)	–	0
3	SiO ₂ –TiO ₂ (8)	–	0
4	SiO ₂ –MgO (5)	–	0
5	MgO (4)	<i>L</i> -proline	16 (<i>S</i>)
6	SiO ₂	<i>L</i> -proline	6 (<i>S</i>)
7	TiO ₂	<i>L</i> -proline	12 (<i>S</i>)
8	ZnO (1)	<i>L</i> -proline	0
9	SiO ₂ –TiO ₂ (8)	<i>L</i> -proline	2 (<i>S</i>)
10	Composite SiO ₂ –Mg(OH) ₂ * <i>L</i> -proline unwashed (6)		18 (<i>S</i>)
11	Composite SiO ₂ –Mg(OH) ₂ * <i>L</i> -proline washed (7)		4 (<i>R</i>)
12	Composite SiO ₂ –TiO ₂ * <i>L</i> -proline unwashed (9)		2.6 (<i>S</i>)
13	Composite SiO ₂ –TiO ₂ * <i>L</i> -proline washed (10)		0
14	Composite ZnO* <i>L</i> -proline unwashed (2)		12 (<i>S</i>)
15	Composite ZnO* <i>L</i> -proline washed (3)		0

amount of active basic sites was found for the SiO₂–Ti–O₂**L*-proline composite after the removal of *L*-proline by washing (samples 8 and 10). These are apparently the oxygen atoms of the oxides, which are Brønsted basic sites.

The addition of individual magnesium oxide to *L*-proline increases its *ee* value of the resultant product from 11 to 16% (Table 2, experiment 5). While the addition of the Si–Mg and Si–Ti double oxides or individual zinc oxide to *L*-proline led to a decrease in *ee* to zero, the use of the corresponding composites permitted an increase in this value. The value of *ee* = 18% was found for composite 6 (experiment 10) obtained by sol-gel synthesis. The (*S*)-enantiomer predominated in virtually all these experiments. The removal of *L*-proline from the composites (samples 3, 6, and 9) led to a decrease in *ee* almost to zero (experiments 11, 13, and 15). These results show that metal *L*-prolinates formed on the surface of oxides can be seen as a chiral inducer of the Biginelli reaction.

Conclusions. We have prepared ZnO**L*-proline, SiO₂–Mg(OH)₂**L*-proline, and SiO₂–TiO₂**L*-proline. IR spectroscopy indicates that the formation of these composites by sol-gel synthesis leads to virtually complete decomposition of the zwitter-ion structure of *L*-proline and formation of a complex with spectral characteristics similar to the metal *L*-prolinate. The changes in the bands for the Si–O and metal–oxygen bonds in the IR spectra of these composites, especially after the removal of *L*-proline, may be related to the formation of a molecular footprint of this organic compound.

The modification of these oxides during their sol-gel synthesis by *L*-proline permits an increase in the amount of *L*-proline molecules incorporated into the composite by several times in comparison with ordinary adsorption. More than tripling of the amount of basic active sites was found in the SiO₂–Ti–O₂**L*-proline composite after removal of *L*-proline. This finding may be ascribed to a new means of formation of the active sites on the surface of these oxides. The addition of metal oxide**L*-proline composites leads to an increase in the enantiomeric excess of the Biginelli reaction product, which may be attributed to the presence of structures on the catalyst surface similar to the metal *L*-prolinates.

Acknowledgment. This work was carried out as part of State Project AAAA-A19-119012290117-6 using the equipment of the Collective Center for Spectroscopy and Analysis of Organic Compounds (TsKP SAOS).

REFERENCES

1. Yu. A. Titova, O. V. Fedorova, G. L. Rusinov, and V. N. Charushin, *Usp. Khim.*, **84**, No. 12, 1294–1515 (2015).
2. J. L. G. Fierro, *Metal Oxides. Chemistry and Applications*, Taylor & Francis Group, New York (2006), pp. 247–300.

3. A. A. Davydov, *IR Spectroscopy of Oxide Surfaces* [in Russian], Nauka, Novosibirsk (1984), pp. 10–66.
4. A. Davydov, *Molecular Spectroscopy of Oxide Catalyst Surfaces*, John Wiley & Sons, Chichester (2003), pp. 27–179, 445–453.
5. R. T. Koodall and K. J. Klabunde, in: *Surface and Nanomolecular Catalysis. Catalysis by Metal Oxides*, Taylor & Francis Group, New York (2006), pp. 48–50.
6. K. Tanabe, *Solid Acids and Bases* [Russian translation], Mir, Moscow (1973), pp. 13–67.
7. O. V. Fedorova, M. S. Valova, Yu. A. Titova,, I. G. Ovchinnikova, A. N. Grishikov, M. A. Uimin, A. A. Mysik, A. E. Ermakov, G. L. Rusinov, and V. N. Charushin, *Kinetika Kataliz*, **52**, No. 2, 234–241 (2011).
8. O. V. Fedorova, O. V. Koryakova, M. S. Valova, I. G. Ovchinnikova, Yu. A. Titova, G. L. Rusinov, and V. N. Charushin, *Kinetika Kataliz*, **51**, No. 4, 590–596 (2010).
9. O. V. Fedorova, Yu. A. Titova, A. Yu. Vigorov, M. S. Toporova, O. A. Alisienok, A. N. Murashkevich, V. P. Krasnov, G. L. Rusinov, and V. N. Charushin, *Catal. Lett.*, **146**, No. 2, 493–498 (2016).
10. L. V. Chopda and P. N. Dave, *Chem. Sci.*, **5**, 5552–5572 (2020).
11. K. S. Atwal, B. S. Swanson, S. E. Unger, D. M. Floyd, S. Moreland, A. Hedberg, and B. C. O'Reilly, *J. Med. Chem.*, **34**, 806–811 (1991).
12. S. DeBonis, J. P. Simorre, I. Crevel, L. Lebeau, D. A. Skoufias, A. Blangy, C. Ebel, P. Gans, R. Cross, D. D. Hackney, R. H. Wade, and F. Kozielski, *Biochemistry*, **42**, No. 2, 338–349 (2003).
13. M. M. Heravi, S. Asadi, and B. M. Lashkariani, *Mol. Divers.*, **17**, 389–407 (2013).
14. E. R. Jarvo and S. J. Miller, *Tetrahedron*, **58**, 2481–2495 (2002).
15. K. Nakamura, R. Yamanka, T. Matsuda, and T. Harada, *Tetrahedron. Asymmetry*, **14**, 2659–2681 (2003).
16. W. Hotz, F. Tanaka, and C. F. Barbas, *Acc. Chem. Res.*, **37**, 580–591 (2004).
17. J. Pandey, N. Anand, and R. P. Tripathi, *Tetrahedron*, **65**, 9350–9356 (2009).
18. G. Brahmachari, Â. Fátima, B. S. Terra, L. S. Netto, and T. C. Braga, *J. Adv. Res.*, **6**, 317–337 (2015).
19. Z. N. Siddiqui, *C. R. Chimie*, **16**, 183–188 (2013).
20. A. Ghorbani-Choghamarani, and P. Zamami, *Chin. Chem. Lett.*, **24**, No. 9, 804–808 (2013).
21. S. J. Bae, S. W. Kim, T. Hyeon, and B. M. Kim, *Chem. Commun.*, 31–32 (2000).
22. S. W. Kim, S. J. Bae, T. Hyeon, and B. M. Kim, *Microporous Mesoporous Mater.*, **44–45**, 523–529 (2001).
23. Zh. An, W. Zhang, H. Shi, and J. He, *J. Catalysis*, **241**, 319–327 (2006).
24. A. N. Murashkevich, *Vestnik Belorussk. Respublikansk. Fond Fundament. Issledovaniy*, **8**, No. 3, 56–66 (2020).
25. P. P. Fedorov, E. A. Tkachenko, S. V. Kuznetsov, V. V. Voronov, and S. V. Lavrishchev, *Neorg. Mater.*, **43**, No. 5, 574–576 (2007).
26. A. N. Murashkevich, O. A. Alisienok, and I. M. Zharskii, *Kinetika Kataliz*, **52**, No. 6, 1–8 (2011).
27. M. S. Valova, O. V. Koryakova, A. N. Maksimovskikh, O. V. Fedorova, A. N. Murashkevich, and O. A. Alisienok, *J. Appl. Spectrosc.*, **81**, No. 3, 422–426 (2014).
28. *State Standard GOST 18307, Silicon Dioxide Powder. Technical Conditions* [in Russian].
29. V. N. Borodin, *Zhurn. Fiz. Khimii*, **51**, 928–929 (1977).
30. A. W. Herlinger and Th. V. Long II, *J. Am. Chem. Soc.*, **92**, 6481–6486 (1970).
31. L. Bellamy, *Infrared Spectra of Complex Molecules* [Russian translation], Inostr. Lit., Moscow (1963), pp. 335–339.
32. F. Boccuzzi, C. Morterra, R. Scala, and A. Zecchina, *J. Chem. Soc. Faraday Trans.*, **77**, No. 2, 2059–2066 (1981).
33. F. Boccuzzi, E. Borella, A. Zecchina, A. Bossi, and M. Camia, *J. Catal.*, **51**, 150–159 (1978).
34. H. Heiland and H. Lüth, *Solid State Commun.*, **5**, 199–202 (1967).
35. D. Lin-Vien, N. Colthup, W. Fateley, and J. Grasselli, *The Handbook of Infrared and Raman Characteristic Frequencies of Organic Molecules*, Academic Press, Boston (1991), pp. 156–157.
36. K. Nakamoto, *IR and Raman Spectra of Inorganic and Coordination Compounds* [Russian translation], Mir, Moscow (1991), pp. 210–223, 274–279, 109.
37. A. R. Oliveira, R. Katla, M. P. D. Rocha, T. B. Albuquerque, C. D. G. Silva, V. L. Kupfer, A. W. Rinaldi, and N. L. C. Domingues, *Synthesis*, **48**, 4489–4494 (2016).
38. R. A. Nyquist and R. O. Kagel, *Infrared Spectra of Inorganic Compounds*, Academic Press, New York–London (1971), pp. 206–207, 220–221, 234–235.